

COUPLED PLASTIC DAMAGE MODEL FOR LOW AND ULTRA-LOW CYCLE SEISMIC FATIGUE

LUCIA G. BARBU^{*}, SERGIO OLLER[†], XAVIER MARTINEZ[†] AND ALEX H.
BARBAT[†]

^{*,†}International Center for Numerical Methods in Engineering (CIMNE)
Universidad Politécnica de Cataluña
Campus Norte UPC, 08034 Barcelona, Spain
e-mail: lgratiela@cimne.upc.edu

Key Words: *LCF, ULCF, Plastic damage model, Seismic fatigue*

Abstract. This paper presents the theoretical framework for a coupled plastic damage constitutive model valid for materials subjected to cyclic loads that lead to low and ultra-low cycle fatigue. Two numerical examples were presented in order to illustrate the behaviour of the model and its capabilities.

1. INTRODUCTION

The fatigue phenomenon produces a loss of material strength as a function of the number of cycles, load amplitude, reversion index, etc. This loss of strength induces the material to inelastic behaviour, micro-cracking followed by crack coalescence, leading to the final collapse of structural parts. When dealing with low and ultra-low cycle fatigue (LCF and ULCF), characterized by levels of stress superior to the elastic limit, this collapse occurs for a number of cycles below 10^5 and it is due to both damage and plasticity effects.

The most common procedures used to simulate LCF and ULCF are based on counting the number of cycles that can be applied to the material for a given plastic strain. Examples of those approaches are the Coffin-Manson rule, or the enhanced rule proposed by Xue [1]. However, one of the main drawbacks of these formulations is that they require regular cycles to predict the material failure and, often, this regularity does not exist. Furthermore, these approaches do not take into account a change in material stiffness that can influence the estimated fatigue life for low cycle fatigue.

This work proposes the coupling of a plastic model with a damage model to simulate Low and Ultra Low Cycle Fatigue. The constitutive model is based on the work of Luccioni et al. [2] for monotonic loads. The hardening behaviour of the material is formulated in terms of the dissipated energy as presented by Martinez et al. in [3]. With this approach, the energy required in each hysteresis cycle by both the damage process and the plastic process is measured, as well as the available remaining energy of the material. Failure takes place when all the fracture energy of the material has been dissipated.

The effect of the accumulation of number of cycles of loading can be taken into account as proposed by Oller et al. in [4]. This implies the incorporation of a new internal variable for the

model, the number of cycles, which affects the damage and plasticity yield surfaces. Furthermore, it can make use of the load-advancing strategy proposed by Barbu et al. in [5] ensuring a reasonable computational time for materials that fail in a range of 10^4 - 10^5 cycles.

2. PLASTIC DAMAGE MODEL FORMULATION

LCF and ULCF mechanical processes cannot be modelled using traditional fracture mechanics and fatigue models because they are often accompanied by large inelastic strains (damage and/or plasticity) which may invalidate stress intensity-based ΔK or ΔJ – type approaches [6]. Furthermore, the induced loading histories are extremely random in the case of ULCF, difficult to adapt to conventional cycle counting techniques such as rain flow analysis [7, 8] or strain life approaches. Finally, ΔK or ΔJ – type methods require an initial sharp crack or flaw, which is absent in many structural details. These limitations, together with the large strain advance finite-element formulation methods, require understanding the underlying ULCF and LCF processes and the development of improved models to predict them.

The study of LCF should start from the basic fact that it is not a phenomenon associated to the classic concept of plasticity. Typically, a progressive loss of strength occurs depending on the number of stress cycles that induces local plasticity and/or damage effects. In addition, all these phenomena are usually coupled with thermal effects.

These phenomena will be simulated with a constitutive model that couples plasticity, driven by a yield function, with a mechanical damage affected by the number of cycles. The damage model takes into account the pore formation and the subsequent coalescence. The Bauschinger effect [9, 10] is taken into account by means of the kinematic hardening incorporated in the plasticity formulation. The strength reduction produced at a very low number of the cycles is a consequence of the softening caused by kinematic effects on the plastic yield function during cyclic plasticity (Bauschinger effect [9,10]). Following these ideas, a phenomenological model is formulated to couple plastic and damage behaviours. This model activates itself with the accumulation of the number of cycles leading to the loss of strength at each point for a wide range of fatigue processes. The decrease of the strength shows a crack in which the total fracture energy available at each point is dissipated. Thus, the structural fracture is expressed as a succession of points that have suffered loss of strength during fatigue.

The coupling between plasticity and damage, together with the addition of the sensibility to the number of cycles in both formulations, provides a general fatigue model capable of working in a wide field, ranging from ultra-low cycle fatigue to high cycle fatigue.

The inclusion of the number of cycles into the plastic and damage formulation, through its internal variables, allows the incorporation of the accumulative damage in the fatigue process, requiring no special or additional constitutive rule [11]. Thus, the constitutive model proposed herein is able to account for non-linear damage accumulation problems that occur when a structural part is subjected to cycles of different load amplitudes and duration (low and high number of cycles).

2.1 Quasi-static elasto-plastic damage model. Mechanical formulation.

The theories of plasticity and/or damage can simulate the material behaviour beyond the elastic range, taking into account the change in the strength of the material through the movement of the yield and/or damage surface (isotropic and kinematic) due to the inelastic behaviour (plasticity and damage) of each point of the solid. However they are not sensitive to cyclic load effects. In this work the standard inelastic theories are modified to introduce the fatigue effect coupled with non-fatigue material behaviour.

It is assumed that each point of the solid follows a damage-elasto-plastic constitutive law (stiffness hardening/softening) [2, 12 and 13] with the stress evolution depending on the free strain variable and plastic and damage internal variables. The formulation proposed herein studies the phenomenon of stiffness degradation and irreversible strain accumulation through the combined effect of damage and plasticity.

Since this work is oriented towards mechanical problems with small elastic strains and large inelastic strains, the free energy additively hypothesis is accepted $\Psi = \Psi^e + \Psi^p$ [14, 15]. The elastic Ψ^e and plastic Ψ^p parts of the free energy are written in the reference configuration for elastic Green strains $E_{ij}^e = E_{ij} - E_{ij}^p$; the last variable operates as a free field variable [2, 13, 15, and 16]. The free energy is thus written as

$$\Psi = \Psi^e(E_{ij}^e, d) + \Psi^p(\alpha^p) = (1-d) \frac{1}{2m^o} [E_{ij}^e C_{ijkl}^o E_{kl}^e] + \Psi^p(\alpha^p) \quad (1)$$

Considering the second thermodynamic law (Clausius-Duhem inequality – [14, 17, 18], the mechanical dissipation can be obtained as [15]

$$\Xi = \frac{S_{ij} \dot{E}_{ij}^p}{m^o} - \frac{\partial \Psi}{\partial \alpha^p} \dot{\alpha} - \frac{\partial \Psi}{\partial d} \dot{d} \geq 0 \quad (2)$$

The fulfilment of this dissipation condition (Equation 2) demands that the expression of the stress should be defined as (Coleman method; see [18])

$$S_{ij} = m^o \frac{\partial \Psi}{\partial E_{ij}^e} = (1-d) C_{ijkl}^o (E_{kl}^e) \quad (3a)$$

Also, from the last expressions, the secant constitutive tensor can be obtained as:

$$C_{ijkl}^s(d) = \frac{\partial S_{ij}}{\partial E_{kl}^e} = m^o \frac{\partial^2 \Psi^e}{\partial E_{ij}^e \partial E_{kl}^e} = (1-d) C_{ijkl}^o \quad (3b)$$

where m^o is the material density, $E_{ij}^e, E_{ij}, E_{ij}^p$ are the elastic, total and plastic strain tensors, $d^{ini} \leq d \leq 1$ is the internal damage variable enclosed between its initial value d^{ini} and its

maximum value 1, α^p is a plastic internal variable, C_{ijkl}^0 and C_{ijkl}^s are the original and secant constitutive tensors and S_{ij} is the stress tensor for a single material point.

2.2 Yield and potential plastic functions

The yield function F^p accounts for the residual strength of the material, which depends on the current stress state and the plastic internal variables and, in the formulation proposed herein, it is sensitive to the fatigue phenomenon. This F^p function has the following form, taking into account isotropic and kinematic plastic hardening (Bauschinger effect [9, 10]):

$$F^p(S_{ij}, \alpha^p) = f^p(S_{ij} - \eta_{ij}) - K^p(S_{ij}, \kappa^p, N) \leq 0 \quad (4)$$

where $f^p(S_{ij} - \eta_{ij})$ is the uniaxial equivalent stress function depending of the current value of the stresses S_{ij} , η_{ij} is the kinematic plastic hardening internal variable, $K^p(S_{ij}, \kappa^p, N)$ is the plastic strength threshold and κ^p is the plastic isotropic hardening internal variable [2, 12, 13]. N is the number of cycles of the stress in the point of the solid and α^p is a symbolic notation for all the plastic variables involved in the process.

The evolution law for the plastic strain is $\dot{E}_{ij}^p = \lambda \frac{\partial G^p}{\partial S_{ij}}$, being λ the consistency plastic factor and G^p the plastic potential.

Kinematic hardening accounts for a translation of the yield function and allows the representation of the Bauschinger effect in the case of cyclic loading. This translation is driven by the kinematic hardening internal variable η_{ij} which, in a general case, varies proportionally to the plastic strain of the material point. One of the laws that define the evolution of this parameter is

$$\dot{\eta}_{ij} = c_k \dot{E}_{ij}^p, \text{ with } c_k = \frac{2}{3} h_k \text{ for Von Mises} \quad (5)$$

where h_k is a material property to be determined by particular tests for the Prager and Melan kinematic hardening [15]. The evolution of isotropic hardening is controlled by the evolution of the plastic hardening function K^p , which is often defined by an internal variable κ^p . The rate equation for these two functions may be defined, respectively, by

$$\begin{aligned} \dot{K} &= \dot{\lambda} \cdot H_k = h_k \cdot \dot{\kappa}^p \\ \dot{\kappa}^p &= \dot{\lambda} \cdot H_k = \dot{\lambda} \cdot \left[h_k : \frac{\partial G}{\partial S} \right] = h_k \cdot \dot{E}^p \end{aligned} \quad (6)$$

where k denotes scalar and \mathbf{k} stands for a tensor function. Depending on the functions defined to characterize these two parameters, different solid performances are obtained.

2.3 Threshold damage function

Onset of damage depends on the current stress state, the internal damage variable and, with the current formulation, it also depends on the number of cycles. The threshold damage function is defined as (see [18, 19])

$$\begin{aligned} F^D(S_{ij}, d) &= f^D(S_{ij}) - K^D(S_{ij}, d, N) \leq 0 \\ G^D(S_{ij}, d) &= g^D(S_{ij}) = cte. \end{aligned} \quad (7)$$

where $f^D(S_{ij})$ is the equivalent stress function in the undamaged space, $K^D(S_{ij}, d, N)$ is the damage strength threshold, and $d = \int_0^t \dot{d} dt$ the damage internal variable.

The evolution of the damage strength threshold is analogous to that of the plastic strength threshold, depending on the internal degradation variable κ^d

$$\begin{aligned} \dot{K}^D &= h_k^d \cdot \dot{\kappa}^d \\ \dot{\kappa}^d &= h_k^d \cdot \dot{d} \end{aligned} \quad (8)$$

In equation 8, h_k^d is a scalar function with scalar arguments and h_k^d is a scalar function with tensorial arguments as shown by [2, 12, and 13].

2.4 Coupled plastic-damaged response and tangent constitutive law

From the simultaneous consistency conditions for the plastic ($\dot{F}^P = 0$) and damage ($\dot{F}^D = 0$) problems, the evolution of the plastic strain and damage variables can be obtained. The secant constitutive law and the stress rate are

$$\begin{aligned} S_{ij} &= (1-d) C_{ijkl}^o (E_{kl} - E_{kl}^p) \\ \dot{S}_{ij} &= \frac{\partial}{\partial t} [(1-d) C_{ijkl}^o (E_{kl} - E_{kl}^p)] = C_{ijkl}^e \dot{E}_{kl} - C_{ijkl}^p \dot{E}_{kl}^p \\ C_{ijkl}^e &= C_{ijkl}^s - \frac{1}{(1-d)} \frac{\partial G^D}{\partial g^D} \left[\left(\frac{\partial g^D}{\partial S_{rs}^0} \right) C_{rsij}^o \right] S_{kl} \end{aligned} \quad (9)$$

Considering the stress rate as $\dot{S}_{ij} = C_{ijkl}^{ep} \dot{E}_{kl}$, the analytical expression of the tangent constitutive tensor is

$$\begin{aligned} C_{ijkl}^{ep} &= C_{ijkl}^e - \frac{C_{ijrs}^s \frac{\partial G^P}{\partial S_{rs}} \frac{\partial F^P}{\partial S_{mn}} C_{mnkl}^e}{-c_k \frac{\partial F^P}{\partial \eta_{tu}} : \frac{\partial G^P}{\partial S_{tu}} - \frac{\partial F^P}{\partial \alpha_r^p} (h_r)_{tu} \frac{\partial G^P}{\partial S_{tu}} + \frac{\partial F^P}{\partial S_{mn}} C_{mnrs}^s \frac{\partial G^P}{\partial S_{rs}}} \end{aligned} \quad (10)$$

2.5 Algorithm for the numerical implementation of the plastic-damaged model

For this model, plasticity and damage equation must be integrated simultaneous. This is done with the following Euler-backward algorithm. Between two-equilibrium configurations t and $t - \Delta t$ the formulation is updated as follows:

$$\begin{aligned} (E_{ij}^p)_t &= (E_{ij}^p)_{t-\Delta t} + \Delta\lambda \cdot \left(\frac{\partial G^p}{\partial S_{ij}} \right)_t \\ (\alpha^p)_t &= (\alpha^p)_{t-\Delta t} + \Delta\lambda \cdot (H(S_{ij}, \alpha^p))_t \\ (\eta_{ij})_t &= (\eta_{ij})_{t-\Delta t} + \Delta\lambda \cdot c_k \cdot \left(\frac{\partial G^p}{\partial S_{ij}} \right)_t \\ (d)_t &= (d)_{t-\Delta t} + \Delta d_t \end{aligned} \quad (11)$$

The stress state is updated according to the secant constitutive law shown in equation 9 and its reduction to the damage and plastic yield surfaces is done simultaneously leading to the following non-linear system of equations:

$$\begin{aligned} H^p(\Delta\lambda_t, \Delta d_t) &= F^p(S_{ij}, \alpha^p) = f^p(S_{ij} - \eta_{ij}) - K^p(S_{ij}, \kappa^p, N) = 0 \\ H^d(\Delta\lambda_t, \Delta d_t) &= F^d(S_{ij}, d) = f^d(S_{ij}) - K^d(S_{ij}, d, N) = 0 \end{aligned} \quad (12)$$

This system of equations can be solved by Newton-Raphson procedure [20]

$$\begin{Bmatrix} \Delta\lambda_t \\ \Delta d_t \end{Bmatrix}_k = \begin{Bmatrix} \Delta\lambda_t \\ \Delta d_t \end{Bmatrix}_{k-1} - \left[\begin{array}{cc} \left(\frac{\partial H^p}{\partial \Delta\lambda} \right)_t & \left(\frac{\partial H^p}{\partial \Delta d} \right)_t \\ \left(\frac{\partial H^d}{\partial \Delta\lambda} \right)_t & \left(\frac{\partial H^d}{\partial \Delta d} \right)_t \end{array} \right]_{k-1}^{-1} \begin{Bmatrix} H^p(\Delta\lambda_t, \Delta d_t) \\ H^d(\Delta\lambda_t, \Delta d_t) \end{Bmatrix}_{k-1} \quad (13)$$

Despite having the analytical expression of the tangent constitutive tensor, equation (10), the calculation of this tensor is extremely costly and, depending on the yield and damage functions used, its approximation does not provide correct results. To overcome this drawback this tensor will be calculated numerically by a perturbation method. This is obtained as

$$C_{ijab}^{ep} = \frac{\delta \dot{S}_{ij}}{\delta \dot{E}_{ab}} \quad (14)$$

with $\delta \dot{E}_{ab}$ an infinitesimal perturbation applied to the mechanical strain tensor, and $\delta \dot{S}_{ij}$ the stress variation produced by the strain perturbation. With this procedure, it is necessary to apply twice $a \times b$ perturbations to obtain the complete tangent tensor. However, despite the computational cost, it provides an accurate approximation that improves the global convergence of the problem [21].

3. PLASTIC DAMAGE MODEL ORIENTED TO FATIGUE ANALYSIS

The effects of a cyclic load on the constitutive behaviour of a material range from the

accumulation of plastic strain in the case of ULCF to the reduction of material stiffness when dealing with high cycle fatigue. LCF induces changes in the material that are a combination of the aforementioned phenomena. In the following the methodology and motivation for taking into account the effects generated by the cyclical load will be presented.

3.1 Ultra-low cycle fatigue

The model is able to account for ULCF effects by incorporating a new law, especially developed for steel materials, that has been designed to reproduce their hardening and softening performance under monotonic and cyclic loading conditions (Figure 1). This law depends on the fracture energy of the material.

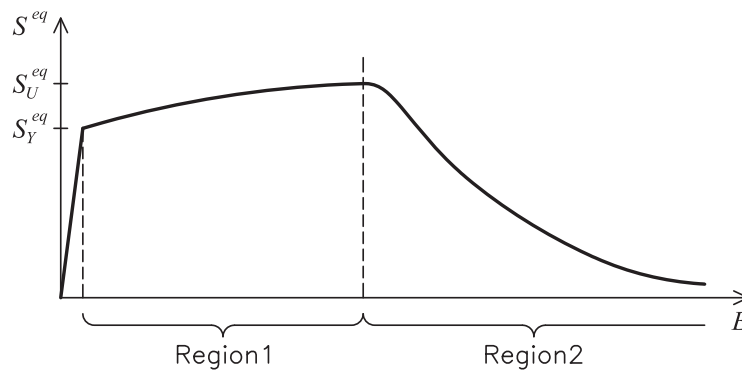


Figure 1: Evolution of the equivalent stress

The equivalent stress state shown in Figure 1 has been defined to match the uniaxial stress evolution shown by most metallic materials. This curve is divided in two different regions. The first region is defined by fitting a curve to a given set of equivalent stress-equivalent strain points. This curve is a polynomial of any given order and is fitted by using the least squares method. The data given to define this region is expected to provide an increasing function, in order to obtain a good performance of the formulation for cyclic analysis.

The second region is defined with an exponential function to simulate softening. The function starts with a null slope that becomes negative as the equivalent plastic strains increases. The exact geometry of this last region depends on the fracture energy of the material. The exact formulation of the constitutive law can be found in Martinez et al. [3].

Characteristic of this type of fatigue is the Bauschinger effect that is taken into account in the constitutive model by combining isotropic hardening with kinematic hardening. The energy dissipated in each hysteresis loop is monitored and failure under cyclical loads is reached when the total available fracture energy of the material is spent.

The plastic damage formulation presented in this paper can be used to improve result accuracy when simulating the softening behaviour under ULCF loads.

3.2 Low cycle fatigue

The behaviour of a material subjected to cyclical loads that induce low cycle fatigue (LCF) exhibits both accumulation of plastic strain and a reduction of stiffness (Figure 2). While

ULCF can be described exclusively by plastic models and HCF by damage models, LCF should be modelled with coupled plastic damage models. It is often difficult to predict at which moment in the material life stiffness reduction begins, since the boundaries between these types of fatigue are rather arbitrary. The model this paper proposes aims at making a contribution in correctly assessing the fatigue life for materials subjected to ULCF and LCF and is particularly effective for the transition zone between these two phenomena.

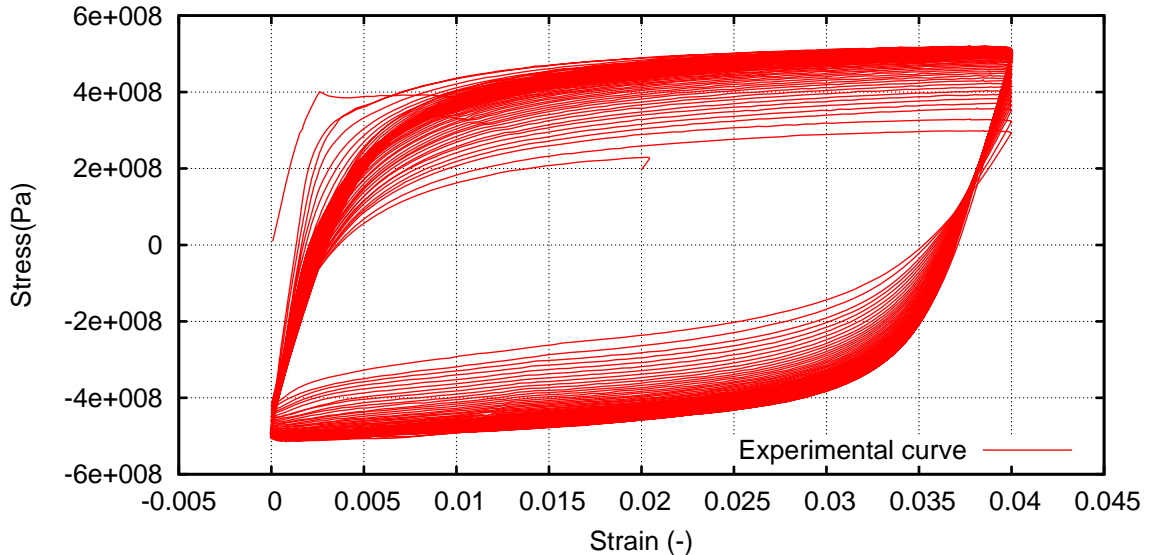


Figure 2: Experimental stress-strain curve for X52 steel [22]

In the context of the hardening law proposed for ULCF, the plastic damage model presented in this work activates itself in the softening region. This is justified by the physical implications behind the damage phenomenon, as damage induces porosity that leads to stress relaxation. This implies that region 1 in Figure 1 is governed by plasticity ensuring that only the cyclical loads that last a long enough number of cycles get to experience damage effects. This is important as the formulation is meant to guarantee that, for a material life clearly in the ULCF range (dozens of cycles or less), the constitutive equations governing should be those of plasticity. By regulating the extension of region 1 with respect to region 2 discrimination is made between materials that exhibit more sensitivity to ULCF with respect to LCF or the opposite.

4. PERFORMANCE OF THE FORMULATION

In the following we included the results obtained for several simulations conducted to illustrate the performance of the formulation presented. These simulations prove the ability of the formulation to characterize mechanical softening behaviour, under monotonic loading conditions. The main aim of all these simulations is to show the response obtained with the proposed constitutive model. Therefore, for the sake of simplicity, and to reduce the computational cost of the simulations, all of them have been conducted on a single hexahedral finite element. The element is fixed in one of its faces and the load is applied to the opposite face as an imposed displacement.

4.1 Simulation of the mechanical performance under monotonic loads – softening behaviour

The first simulation presents the capabilities of the formulation when dealing with materials that exhibit softening behaviour. The material characteristics are given in Table 1.

Table 1: Material characteristics

Young Modulus	$2.01 \cdot 10^5$ MPa
Poisson Modulus	0.30
Elastic Stress (σ_y^{eq})	838.9 MPa
Fracture Energy	0.1 MN·m/m ²

Figure 3 shows the evolution of the stress for the plastic damage model as compared with the same simulation conducted with a classic plasticity model and with a classical scalar damage model such as that proposed by Kachanov [23].

Three different simulations were made with the coupled model. The first one assumes equal distribution of energy between the two interconnected phenomena: 50% for damage and 50% for plasticity. A different one was made with 10% for damage and 90% for plasticity and the last one allotted 90% for damage and 10% for plasticity. Unloading was made at approximately the middle of the loading history in order to observe better the material behaviour. For the numerical simulations using the two uncoupled models, the entire available fracture energy was used (100%).

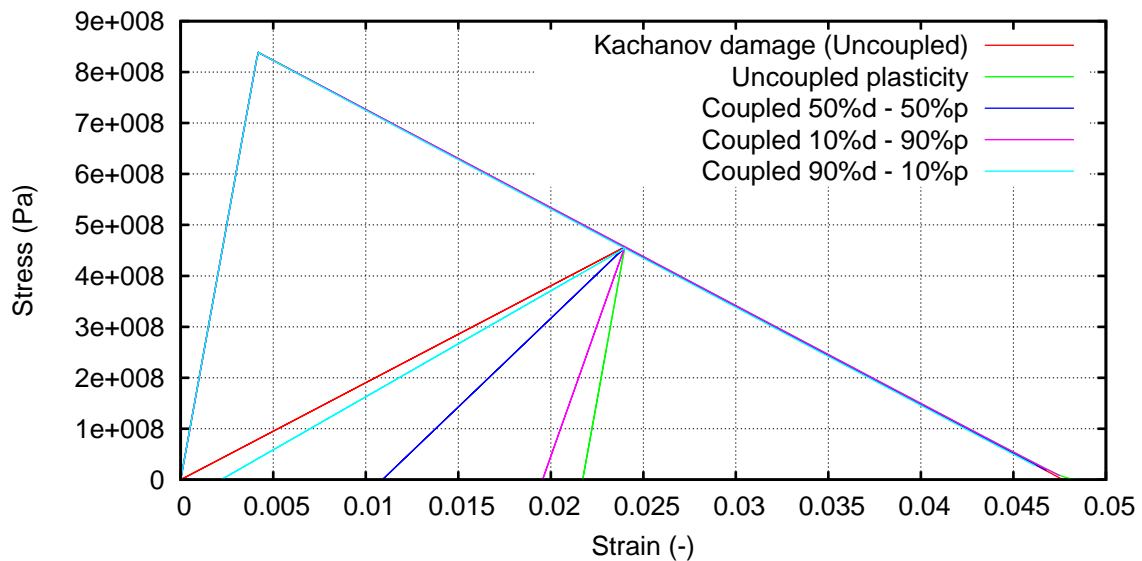


Figure 3: Stress evolution for the plastic damage model as compared to the classical plasticity and damage models

It can be seen in Figure 3 that, unless the material is unloaded, the behaviour is the same in all the simulations ran. When unloading, the loss of stiffness and the accumulated plastic strain are in accordance with the percentage of energy given to each one of the models. For

instance, for the simulation performed with 50% of the energy in damage and 50% in plasticity, when the material is completely unloaded the plastic strain corresponding to the coupled model is 50% of the plastic strain of the uncoupled plastic model. Also, the stiffness reduction is only 50% of the stiffness loss corresponding to the uncoupled damage model.

Both internal variables of the model, κ^p and d , reach a unitary value at the end of the simulation. This states that the energy available for each process has been spent and that, on the whole, all the available internal energy of the material has been dissipated

$$G_f = \underbrace{(100 - p\%) \cdot G_f}_{G_f^p} + \underbrace{p\% \cdot G_f}_{G_f^d}$$

$$1 = d \cdot \frac{p\%}{100} + \kappa^p \cdot \left(1 - \frac{p\%}{100}\right), \text{ with } 0 \leq d \leq 1 \text{ and } 0 \leq \kappa^p \leq 1 \quad (15)$$

where $p\%$ is the participation factor for the damage process.

4.2 Simulation of the mechanical performance under cyclic loads – hardening softening behaviour

In this section, the material behaviour will be simulated with the hardening-softening law described in [3]. Both kinematic and isotropic hardening is taken into account. The hardening region will make use of the plasticity formulation described in [3], while the softening region will be described with the formulation presented in this paper. The transition from one constitutive formulation to the other is done automatically at the material points that have reached softening. In Table 2 the material properties used for this simulation are presented.

The fracture energy available for the coupled model is inherited as output from the plastic model. The input is the total available fracture energy along with all the other characteristics of the material, kinematic coefficients and the equivalent plastic deformation at which softening starts in the uniaxial experimental stress-strain curve. The model is highly sensible to the fracture energy available to the damage model.

Table 2: Mechanical properties of steel

Young Modulus	$1.95 \cdot 10^5$ MPa
Poisson Modulus	0.30
Elastic Stress (σ_Y^{eq})	380 MPa
Plastic Strain Softening (E_2^p)	50 %
C1 kinematic hardening	$6.0 \cdot 10^4$ MPa
C2 kinematic hardening	400
Fracture Energy	15.0 MN·m/m ²

For this simulation, the Friederick – Armstrong non-linear kinematic hardening was used. Figure 4 shows the stress-strain curve for a cyclic load with strain amplitude of 5% and a reversion factor equal to 0. The first curve shows the material behaviour when using the proposed plastic damage model in softening. Only 1% of the available internal energy for the

softening branch was directed in damage. The second curve was obtained by using the plasticity formulation presented in Martinez et al. [3]. A progressive reduction in stiffness can be observed from cycle to cycle when the proposed model is used.

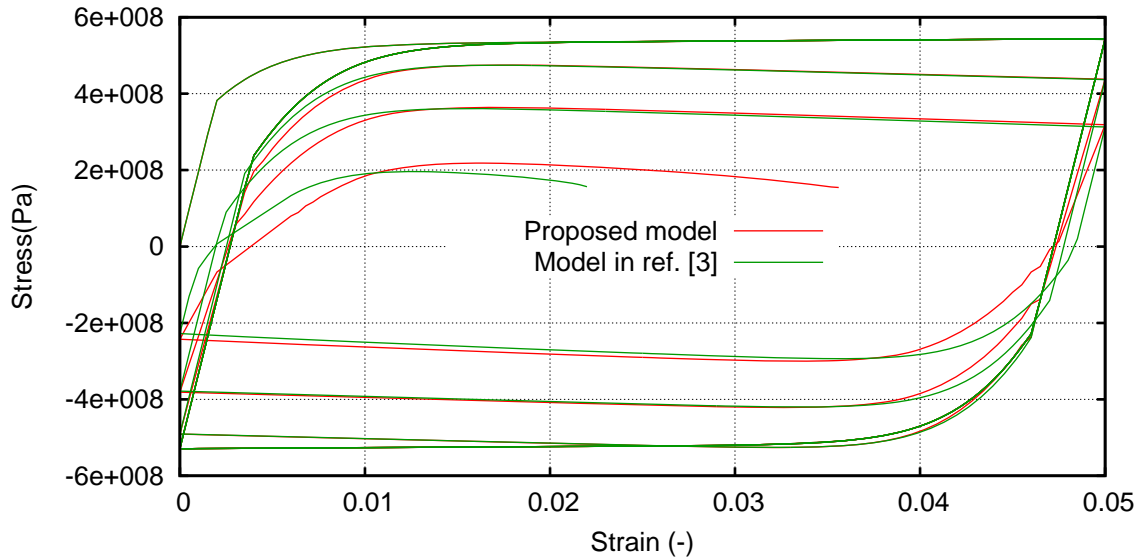


Figure 4: Stress strain curve for the proposed model compared with that of Martinez et al. [3].

5 CONCLUSIONS

This paper has proposed the formulation for a constitutive model that couples plasticity with damage. The model is energy based and the material performance is determined by the amount of energy dissipated by plasticity and by damage. The formulation has been implemented to work in the softening regime as damage is a softening process. This model has been applied to the simulation of ULCF and LCF, improving the softening behaviour of an exclusively plastic formulation.

Acknowledgements: This work has been supported by the Research Fund for Coal and Steel through the ULCF project (RFSR-CT-2011-00029), by the European Research Council under the Advanced Grant: ERC-2012-AdG 320815 COMP-DES-MAT "Advanced tools for computational design of engineering materials", by the research collaboration agreement established between Abengoa Research and CIMNE and by the Spanish Government program FPU: AP2010-5593.

REFERENCES

- [1] Xue, L. A unified expression for low cycle fatigue and extremely low cycle fatigue and its implication for monotonic loading, *Int. J. Fatigue* (2008) **30**:1691-1698.
- [2] Luccioni, B., Oller, S. and Danesi, R. Coupled plastic-damage model, *Computer Methods in Applied Mechanics and Engineering* (1996) **129**:81-90.
- [3] Martinez, X., Oller, S., Barbu, L. and Barbat, A. Analysis of ultra-low cycle fatigue problems with the Barcelona plastic damage model, *Computational Plasticity XII. Fundamentals and Applications* (2013) 352 – 363, ISBN 978-84-941531-5-0.

- [4] Oller, S., Salomón, O. and Oñate, E. A continuum mechanics model for mechanical fatigue analysis, *Computational Materials Science* (2005) **32**:175-195.
- [5] Barbu, L.G., Oller, S., Martinez, X. and Barbat, A. Stepwise advancing strategy for the simulation of fatigue problems, *Computational Plasticity XII. Fundamentals and Applications* (2013) 1153 – 1164, ISBN 978-84-941531-5-0.
- [6] Paris, P., Erdogan, F. A Critical Analysis of Crack Propagation Laws – *ASME, J. Basic Engrg.* (1963) **85**: 528-534.
- [7] Miner, M. Cumulative damage fatigue- *J. App. Mech* (1945) **12**:159-164.
- [8] Tatsuo, E., Koichi, M., Kiyohumi, T., Kakuichi, K. and Masanori, M. Damage evaluation of metals for random of varying loading -Three aspects of rain flow method. *Mechanical behavior of materials, Symp. Proc., Soc. Materials Scientists*, Kyoto, Japan, Aug. 21–24, 1974.
- [9] Chun, B.K., Jinna, J.T. and Lee J.K. Modeling the Bauschinger effect for sheet metals, part I: theory. *International Journal of Plasticity* (2002) **18**: 571–595.
- [10] Kassner, M.E., Geantil, P., Levine, L.E. and Larson B. C. Backstress, the Bauschinger Effect and Cyclic Deformation. *Materials Science Forum* (2009) **604-605**: 39-51. Trans Tech Publications, Switzerland.
- [11] Suero, A. and Oller, S. *Tratamiento del Fenómeno de Fatiga Mediante la Mecánica de Medios Continuos*, Monografía CIMNE Nº 45 (1998), Barcelona.
- [12] Lubliner, J., Oliver, J., Oller, S. and Oñate E. A plastic-damage model for concrete, *International Journal of Solids and Structures* (1989) **25**(3):299-326.
- [13] Oller, S. *Modelización Numérica de Materiales Friccionales* - Monografía CIMNE Nº 3 – Barcelona (1991).
- [14] Lubliner, J. On thermodynamics foundations of non-linear solid mechanics - *Int. Journal non-linear Mechanics* (1972) **7**: 237-254.
- [15] Lubliner, J. *Plasticity Theory* - Macmillan Publishing, U.S.A. (1990)
- [16] Green, A. and Naghdi P. A general theory of an elastic-plastic continuum - *Arch. Rational Mech. Anal* (1964) **18**:251-281.
- [17] Malvern, L. *Introduction to the Mechanics of Continuous Medium* - Prentice Hall USA. (1969)
- [18] Maugin, G. *The Thermomechanics of Plasticity and Fracture*. Cambridge University Press (1992).
- [19] Simo, J. and Ju, J. Strain and stress based continuum damage models – I Formulation. *Int. J. Solids Structures* (1987) **23**: 821-840.
- [20] Zienkiewicz, O. C. and Taylor, R. . *The Finite Element Method*, 5Th Ed , V 1 and 2, Butterworth-Heinemann, (2000).
- [21] Martinez, X., Oller, S., Rastellini, F. and Barbat, A. A numerical procedure simulating RC structures reinforced with FRP using the serial/parallel mixing theory, *Computers and Structures* (2008) **86** (15-16):1604-1618.
- [22] R. Natal and A. de Jesus, “Monotonic and Low Cycle Fatigue Behaviour of X52 Steel”, *private communication*, (2012).
- [23] Kachanov, L.M. “*Introduction to continuum damage mechanics*”, Martinus, Nijhoff Publisher, Boston- Dordrecht, (1986).